Spatial and Spatio-temporal Epidemiology 45 (2023) 100568

Contents lists available at ScienceDirect

Spatial and Spatio-temporal Epidemiology

journal homepage: www.elsevier.com/locate/sste

Original research

Spatio-temporal model to investigate COVID-19 spread accounting for the mobility amongst municipalities

Chellafe Ensoy-Musoro [a,1], Minh Hanh Nguyen [a,1,*], Niel Hens [a,b], Geert Molenberghs [a,c], Christel Faes [a]

[a] Interuniversity Institute for Biostatistics and statistical Bioinformatics, Data Science Institute, Hasselt University, Belgium
[b] Centre for Health Economics Research and Modelling of Infectious Diseases (CHERMID), Vaccine & Infectious Disease Institute (VAXINFECTIO), University of Antwerp, Belgium
[c] Interuniversity Institute for Biostatistics and statistical Bioinformatics, KU Leuven, Belgium

ARTICLE INFO

Keywords:
COVID-19
Mobility
Stochastic prediction
Spatio-temporal dynamic model

ABSTRACT

The rapid spread of COVID-19 worldwide led to the implementation of various non-pharmaceutical interventions to limit transmission and hence reduce the number of infections. Using telecom-operator-based mobility data and a spatio-temporal dynamic model, the impact of mobility on the evolution of the pandemic at the level of the 581 Belgian municipalities is investigated. By decomposing incidence, particularly into within- and between-municipality components, we noted that the global epidemic component is relatively more important in larger municipalities (e.g., cities), while the local component is more relevant in smaller (rural) municipalities. Investigation of the effect of mobility on the pandemic spread showed that reduction of mobility has a significant impact in reducing the number of new infections.

1. Introduction

The rapid spread of COVID-19 worldwide led to various non-pharmaceutical interventions being implemented by different countries to limit transmission and hence reduce the number of infections (Anderson et al., 2020). Social distancing, mask and shield wearing mandates, and case isolation, quarantine measures have been widely used to limit local transmission and protect vulnerable groups (Liu et al., 2021). The day after WHO declared COVID-19 a pandemic, Belgium went into lockdown with strict measures implemented (Crisiscentrum, 2021). This resulted in significant mobility reductions in the period of March–April 2020 with non-essential business and offices closed. Working from home also became the norm, and was mandatory when possible.

Previous studies evaluating the connection between human mobility and transmission of SARS-CoV-2 have revealed a clear association between mobility restrictions and lower COVID-19 incidence (Badr et al., 2020; Gatalo et al., 2020; Kraemer et al., 2020; Nouvellet et al., 2021). Reduced social contact patterns were also found to impact the virus transmission (Coletti et al., 2021; Zhang et al., 2020). Although these restrictions were found to be highly effective early in the pandemic (Gatalo et al., 2020), many countries are experiencing continued or resurgent widespread transmission of SARS-CoV-2 (World Health Organization, 2021). In Belgium, as in many countries, consecutive waves have been experienced in late 2020, 2021 and to a lesser extent in 2022, which resulted into lockdown measures with time-varying stringency.

Understanding how mobility, and especially the connectivity amongst regions, impacts the COVID-19 spread and how it contributed to the observed spatial dynamics is important in evaluating the effectiveness of these lockdown measures. This has been studied in the past — including, for example, for the 2009 H1N1 pandemic (Bajardi et al., 2011) and the West Africa Ebola epidemic (Peak et al., 2018). For the case of COVID-19, the use of mobile network data (Badr et al., 2020; Gatalo et al., 2020; Pullano et al., 2020; Slater et al., 2022), Google and Apple mobility data (Cot et al., 2021), and social media data (Zeng et al., 2021) have been explored as a method to describe the connectivity amongst regions and to induce spatial dependence.

In this paper, we use mobile phone data to describe the connectivity amongst areas and study the impact of this connectivity on the spread of COVID-19 during the second wave of the pandemic in 2020. We evaluate how connectivity amongst areas influenced the spatio-temporal spread in Belgium by measuring the effect of between-municipality transmission and simulating scenarios with different mobility levels. The methods used for the spatio-temporal epidemic spread model are

* Corresponding author.
E-mail addresses: minhhanh.nguyen@uhasselt.be (M.H. Nguyen), christel.faes@uhasselt.be (C. Faes).
[1] Shared first authorship.

https://doi.org/10.1016/j.sste.2023.100568
Received 25 June 2022; Received in revised form 25 November 2022; Accepted 12 January 2023
Available online 8 February 2023

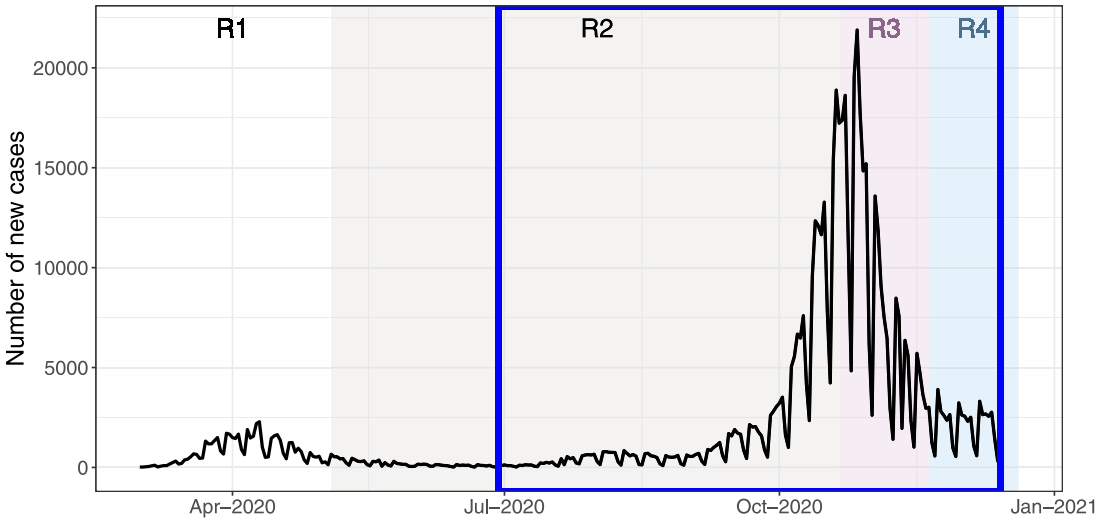

Fig. 1. Daily total COVID-19 cases in Belgium in 2020. The blue square represents the data for the second (Fall) wave used in this paper. R1–R4 shaded areas represent the period of specific testing regulations.

presented in Section 2. Section 3 summarizes the results of the analysis. Section 4 concludes with a discussion.

2. Data and methods

In this section, we first describe the data sources used, and then present a data-driven modeling approach to investigate the contribution of mobility on the spread of COVID-19.

2.1. Case data

The daily numbers of COVID-19 positive tests for each of the 581 municipalities in Belgium were obtained from Sciensano, the Belgian institute for public health (Sciensano, 2021). The overall case time series from 1 March until 13 December 2020 is shown in Fig. 1, which shows a slight bump during the summer period and then a fast increase in October. Note that the first wave in March–April 2020, in spite of its severity, hardly shows up because of limited testing capacity and hence restrictive testing (FOD Volksgezondheid, 2021). During this period, testing was only performed for hospitalized patients and health-care workers (denoted as regulation 1, R1 in Fig. 1). After this period, testing capacity increased substantially as testing was free for anyone with symptoms or who had made a high-risk contact (regulation 2, R2). In the fall of 2020, at the moment that the number of cases was highest, there was too much pressure on the testing capacity, and the testing (R3) was temporarily limited to those with symptoms. After some weeks, testing was again made available to anyone with symptoms, a high-risk contact or for traveling (R4). Table S1 in the Supplemental Materials specifies the periods over which each regulation was in place.

For the purpose of this paper, we use data from 29 June 2020 to 13 December 2020, which captures the Summer 2020 flare-up and the second (Fall) wave of the epidemic. A weekend effect is apparent in the plot. The spatial distributions of the cases during some selected weeks in August, October, and November 2020 are shown in Fig. 2.

2.2. Mobility data

To examine connectivity between municipalities in Belgium, aggregated data from mobile network activity was obtained as from 12 March 2020. For the purpose of this investigation, we use the data from 29 June 2020 onwards. This provides data on the daily total time customers registered with the telecom provider, while residing in municipality j and being active in municipality $i \neq j$. No activity logged for j to i on a specific day means the two municipalities are not 'connected' on that day. Note that the data mainly reflect adults' mobility. Since most young children are accompanied by an adult, this data is implicitly taking into account some of the mobility of children. Yet, the share of which is unknown.

Using the mobile network data, we calculated a daily 7-day moving average of the proportion of time spent in a municipality. This produces a matrix $\boldsymbol{W}_t$ for time t, of dimension 581 × 581, which is a non-symmetric matrix reflecting the commuting behavior of individuals. Figs. 3 and S1 show what the matrices look like for two particular weeks. The y-axis in the plot reflects the municipality of origin (j), while the x-axis corresponds to the destination municipality (i).

2.3. Spatial dynamic model

Let $Y_{i,t}$ be the number of confirmed COVID-19 cases in municipality i on day t, which we model as a Poisson or negative binomial distributed random variable with mean $\mu_{i,t}$ (and overdispersion parameter ψ, for a negative binomial variable). Assuming that the current number of new infections $Y_{i,t}$ depends on the (series of) past observations $Y_{i,t-d}$, $d = 1, \ldots, D$ with up to $D = 14$ days being considered, our model is formulated as:

$$[Y_{i,t}|Y_{t-1}, \ldots, Y_{t-d}] \sim \text{Poi}(\mu_{i,t})$$

or

$$[Y_{i,t}|Y_{t-1}, \ldots, Y_{t-d}] \sim \text{NegBin}(\mu_{i,t}, \psi),$$

with $Y_{t-l} = \{Y_{1,t-l}, \ldots, Y_{M,t-l}\}$ the set of confirmed cases at time $t-l$. The conditional variance for the negative binomial is given by $\mu_{i,t}(1+\mu_{i,t}\psi)$ with an unknown overdispersion parameter $\psi > 0$. The conditional mean μ_{it} is modeled as in Held et al. (2005) as:

$$\mu_{i,t} = \epsilon_{i,t} + \lambda_{i,t}\sum_{d=1}^{D} u_d Y_{i,t-d} + \phi_{i,t}\left(\sum_{d=1}^{D}\sum_{j\neq i} u_d w^*_{j,i,t-d} Y_{j,t-d}\right), \quad (1)$$

which is the sum of an endemic component $\epsilon_{i,t}$, which captures infections arising from sources other than past observed cases, a local epidemic component $\lambda_{i,t}$, measuring the effect of within-municipality transmission, and a global epidemic term $\phi_{i,t}$ measuring the effect of between-municipality transmission due to mobility. The three parameters $\epsilon_{i,t}$, $\lambda_{i,t}$, and $\phi_{i,t}$ are constrained to be non-negative and modeled as a natural log-transformed linear combination of different covariates.

The first term, the endemic component $\epsilon_{i,t}$, is modeled as

$$\log(\epsilon_{i,t}) = \alpha^{(\epsilon)} + \beta^{(\epsilon)}\text{WE}_t + \log\left(\frac{N_i}{N}\right), \quad (2)$$

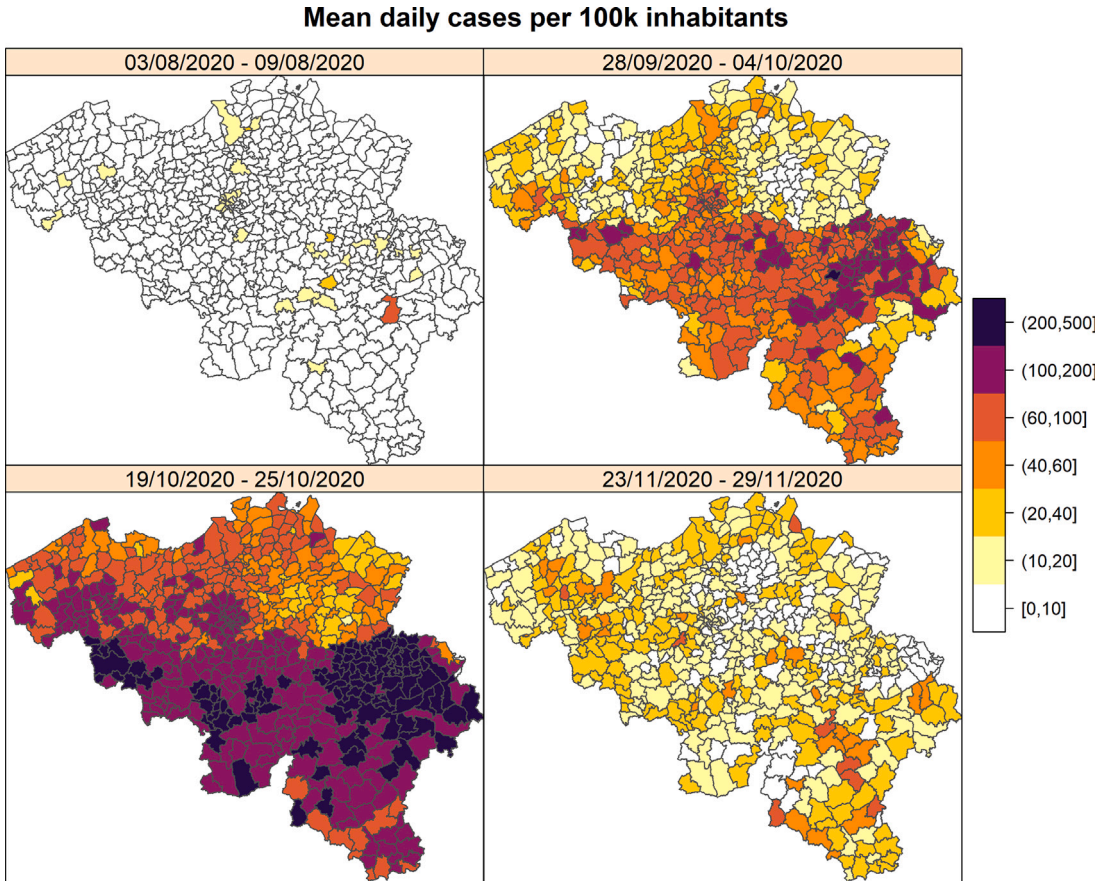

Fig. 2. Mean daily incidence per 100,000 individuals in Belgium for some selected weeks, for the 581 municipalities.

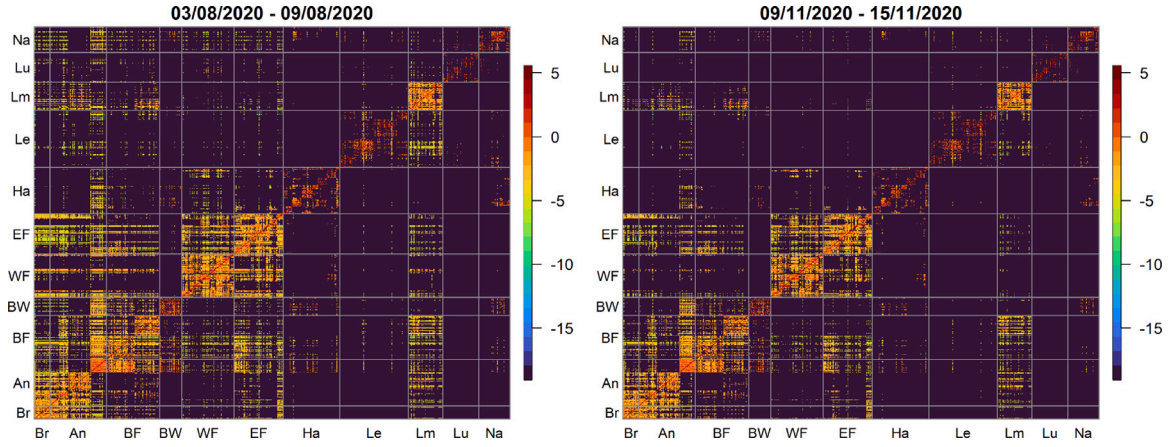

Fig. 3. Log-mean percentage time spent in a municipality for specific weeks based on a 7-day moving average. The y-axis represents the origin while the x-axis is the destination. Different municipalities are grouped according to the 11 provinces in Belgium (An: Antwerp; BF: Brabant Flamand; Br: Brussels; BW: Brabant Wallon; EF: East Flanders; Ha: Hainaut; Le: Liège; Lm: Limburg; Lu: Luxembourg; Na: Namur; WF: West Flanders).

where $\alpha^{(\epsilon)}$ is a constant baseline endemic coefficient and $\beta^{(\epsilon)}$ is the coefficient for the weekend effect, WE_t. The endemic term is weighed by an offset, i.e., the population proportion N_i/N of municipality i.

The second term, representing the local epidemic or within-municipality component, $\lambda_{i,t}$, is modeled as

$$\log(\lambda_{i,t}) = \alpha_i^{(\lambda)} + \beta^{(\lambda)}\mathrm{WE}_t + \gamma^{(\lambda)}\log(N_i) + \sum_k \delta_k^{(\lambda)} \mathbf{1}_{\{t \text{ is under regulation } k\}}(t). \quad (3)$$

Here, we assume either a constant baseline epidemic effect $\alpha_0^{(\lambda)}$ or a municipality-specific effect $\alpha_i^{(\lambda)} \sim \mathrm{N}(\lambda_0, \tau^2)$, allowing some municipalities to be above or below the national average in terms of the ongoing infection risk. It may capture such effects as population density or socio-economic composition, that do not explicitly enter the model's covariate function. The population size was used as a covariate along with two time-dependent covariates: the indicator for weekend day and indicators for the testing regulations ($\mathbf{1}_{\{t \text{ is under regulation } k\}}$). Testing regulation (regulation) came into the model as a covariate to account for the variability in the number of recorded cases due to different testing strategies that Belgium has implemented throughout the pandemic.

The third term represents the mobility component, $\phi_{i,t}$, and is modeled as

$$\log(\phi_{i,t}) = \alpha_i^{(\phi)} + \beta^{(\phi)}\mathrm{WE}_t + \gamma^{(\phi)}\log(N_i) + \sum_k \delta_k^{(\phi)}\mathbf{1}_{\{t \text{ is under regulation } k\}}(t). \tag{4}$$

Similar covariates to that of the second term are incorporated here.

The normalized Poisson weights u_d in (1) represent the probability for a serial interval of up to D days, i.e., the average time in days between symptom onset in an infectious individual and symptoms emerging in a newly infected individual when both are in close contact.

The weights $w^*_{j,i,t}$ describe the connective strength for all pairs of municipalities. Note that we can distinguish between two types of connectivity, related to the movement of a visitor and of someone returning home. The visitor movement is given by the matrix $\boldsymbol{V}_t = \boldsymbol{W}_t$ with elements $w_{j,i,t}$ described by the mobility data, taking the origin municipality as j and the destination municipality as i, while the movement of someone returning home is given by the transpose of this matrix: $\boldsymbol{R}_t = \boldsymbol{W}_t^T$, thereby assuming that a customer spotted in the destination municipality will travel back to the origin municipality at the end of the day. For $i = j$, $w_{j,i,t} = 0$. Based on this, the following choices are made for the weights $w^*_{j,i,t}$:

- **Time varying connectivity.** Using the visitor mobility $W^*_t = V_t$ or the sum of the visitor and return mobility $W^*_t = V_t + R_t$. While the first is an asymmetric connectivity matrix, the second version is symmetric.
- **Fixed connectivity.** A constant weight by taking the mean across the investigated time points. Both the visitor mobility and visitor and return mobility as above are investigated.
- **Smoothed connectivity.** A daily, 7-day average weight:

  $$w^*_{j,i,t} = \frac{1}{7}\sum_{d=0}^{6} w_{j,i,t-d}$$

  based on either the visitor mobility matrix or the visitor and return mobility. This matrix smooths out the mobility trend across a 7-day period.
- **Transformed connectivity.** A transformation of the weights is also investigated assuming a power transformations of the weight, $w^*_{j,i,t} = w^p_{j,i,t-d}$, with $p \in (0, 3]$. A fine grid of powers p with a bin width of 0.05 was used to select the best transformation.

Our approach to construct the mobility weight is novel because it can reflect the change in connectivity between municipalities over time. In addition, while the traditional approach bases the weights on the distance (or order) amongst areas, we define weights based on the observed knowledge of actual connectivity amongst regions.

2.4. Inference

Models were selected based on the lowest Akaike's Information Criteria (AIC) (if random effects were not present) or the lowest logarithmic score (if random-effects are present). The logarithmic score measures the predictive performance of our model and is calculated as minus the logarithm of the predictive distribution evaluated at the observed count (Czado et al., 2009).

Parameter inference is performed using maximum likelihood estimation in the R package `surveillance` (version 1.18, Meyer et al., 2017; Bracher and Held, 2020) and R package `gnm` (version 1.1-1, Turner and Firth, 2020) under R version 4.0.2. This allows us to calculate the contribution to the incidence in each region owing to the intrinsic, within-region and between-region autoregressive terms.

Model predictions were carried out by plugging parameter estimates into the fitted model. A one-day-ahead prediction and a two-week forecast was investigated to assess model fit and the impact of mobility. Dynamic stochastic simulation was done wherein we used the one-day ahead forecast ($\mu_{i,t+1}$) to sample from the Negative Binomial distribution and use this sampled count as input for forecasting the next time point ($\mu_{i,t+2}$).

3. Results

3.1. Model selection of epidemic model

A comparison of different lag values ($d = 1, \ldots, D$ with up to $D = 14$ days) and different formulations of the mobility weight indicates a lag of 7 days to fit best, along with using a fixed mobility weight, instead of a 7-day moving average mobility weight. To further improve model fit, a power transformation was applied to the weight matrix. Fig. 4 shows that the 0.9 power-transformed non-symmetric visitor weight matrix fits the data best. Using the symmetric $V + R$ matrix did not improve model fit. Note that, while the model can account for time-varying connectivity amongst regions, the simpler constant connectivity matrix is better in this analysis. This is in line with the limited impact of restriction measures on mobility during the study period (Fig. 3), while much stronger restriction measures in April 2020 reduced the connectivity of more distant regions much more (Figure S1). In addition, this indicates that small day to day fluctuations in mobility are not of importance for the spread of the epidemic, but rather the overall connectivity amongst regions.

Incorporation of random effects in the three components was also investigated to capture municipality-specific differences in transmission rate. Table S2 shows estimates of the best model from above (Model 1), the best model with a random within-municipality effect (Model 2), and the best model with a random between-municipality effect (Model 3). The model with random endemic intercept was also fitted but did not improve the fit and a model with random effects in the 3 components simultaneously resulted in convergence and estimation issues.

Given that the best model (Model 3) consisted of a random between-municipality effect signals the importance of the municipality-specific propensity for disease transmission from importation of new cases. Supplementary Figure S2 maps out the random effects estimates. While it is clear that there is heterogeneity amongst areas, as some areas have higher propensity than others, there is no clear spatial trend observed. Indeed, transmission from imported cases is a complex interplay between different factors that we have not studied in this analysis.

3.2. Component contributions and model fit

The choropleth maps (to be interpreted together) in Fig. 5 show the contribution to disease incidence of the within- and between-municipality autoregressive parts of the model (the endemic component is not shown because of its negligible contribution). The within-municipality map identifies areas for which the epidemic evolution was primarily driven by a local epidemic process. The between-municipality map indicates regions in which incidence is primarily driven by spread of cases via mobility. This pertains to the susceptibility of each municipality to transmission via importation of new cases. From these maps, it can be observed that in the southern part of the country (Walloon Region), the within-municipality spread is somewhat more important that the between-municipality spread; while in northern part of the country (Flemish Region) the importance of the two varies a lot from municipality to municipality. This can be due to the fact that the Walloon Region is less densely populated as compared to the Flemish Region and to different contact patterns among their inhabitants.

Figs. S3 and S4 show how the within- and between- contributions change over time. It shows the important role of the between-municipality transmission in the summer period and during the early stage leading up to the second wave (from July until mid October), while the within-municipality transmission was more important from mid-October until end of November (which is the period of lockdown). Time-series plots of the three model components are shown in Fig. 6

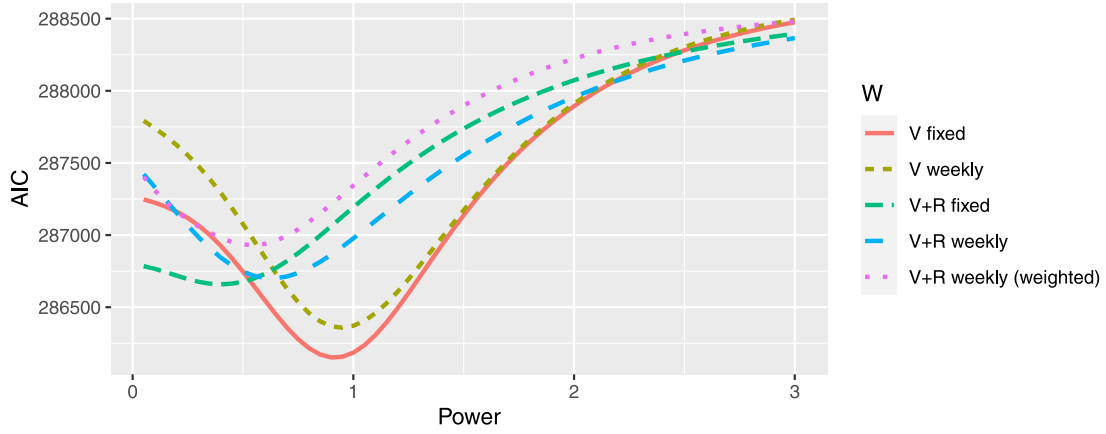

Fig. 4. Model selection: Comparison of different power transformations for the mobility weight matrix. V refers to visitor matrix, $V + R$ refers to the symmetric visitor + return matrix.

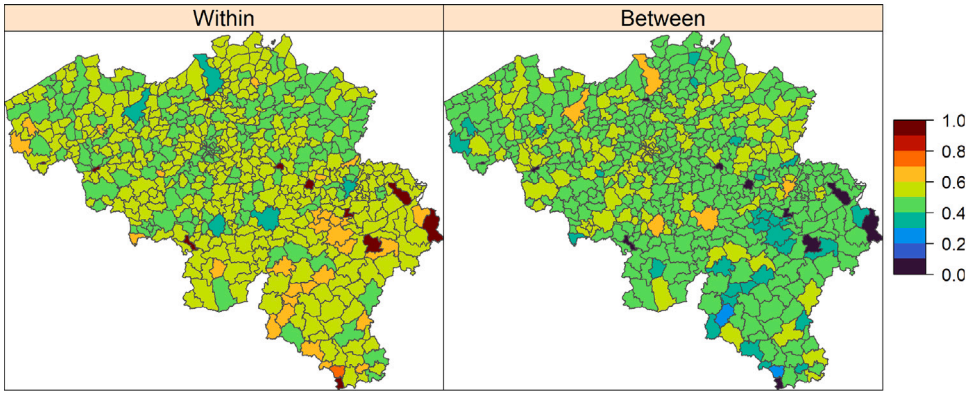

Fig. 5. Contribution of the within- and between-municipality infection rates as a proportion of overall incidence.

for some selected municipalities. It shows that the importance of the epidemic spread between municipalities as compared to within municipalities is more important in large cities, while the epidemic spread within the municipality is more important in small municipalities.

Additionally, one-step ahead predictions (retrospective) and 2-week forecasts for selected municipalities from the best model are made to investigate the predictive performance of the model. These are presented in Figure S5, and plots show good model fit.

3.3. Effect of mobility

Finally, to better understand the impact of mobility amongst municipalities on the epidemic spread, different scenario analyses were investigated. Three scenarios were investigated via stochastic simulation as from October 19: (1) assuming the mobility pattern as observed in October–December, (2) assuming a low mobility pattern (similar as the mobility pattern in April during the first, and most strict, lockdown (see Figure S1), and (3) no mobility between municipalities, which means no connectivity at all between different municipalities. Confirmed cases up to 18 October were used as initial values for the simulation. Fig. 7 shows the results of the scenario analyses. The actual observed mobility describes the time evolution of the epidemic well, with the number of confirmed cases raising to around 500K (Figure S6). Results of the second scenario, assuming a reduction of mobility similar as to how it was during the lockdown period in April 2020, could have greatly reduced the number of new infections, with a stabilization at around 300K confirmed cases. The third scenario, assuming no mobility among regions is an unrealistic scenario, but helps understanding the importance of mobility in sustaining the pandemic, as this scenario shows that without between-municipality mobility the epidemic spread would quickly fade out.

Similar conclusions can be drawn based on the simulation results at municipality level, but in addition show that the impact of reducing the mobility would be largest for the more populated areas. Figure S7 shows the simulation results for some selected (small, medium and large) municipalities. In line with previous results, it is observed that a stricter lockdown, reducing the mobility, would have largest impact in the more populated areas such as in the cities of Antwerp, Brussels, Charlerloi and Liège.

4. Discussion

Using telecom-operator-based mobility data, ranging over 29 June to 13 December 2020 and a spatio-temporal dynamic model, the impact of mobility on the evolution of the epidemic at the level of the 581 Belgian municipalities is investigated. The model allows for separating the municipality-level case number evolution into relevant components: (a) an endemic component, (b) a within-municipality local epidemic component, and (c) a between-municipality mobility driven component.

By decomposing incidence particularly into the within- and between-municipality components, we show that the second-wave of the COVID-19 epidemic in Belgium was highly driven by between-municipality transmission. This was seen as one of the initial driving forces of the epidemic, apart from other factors such as higher exposure due to contact behavior, with some municipalities showing more susceptibility to this mobility-induced transmission. It is noteworthy that this global epidemic component is relatively more important in larger

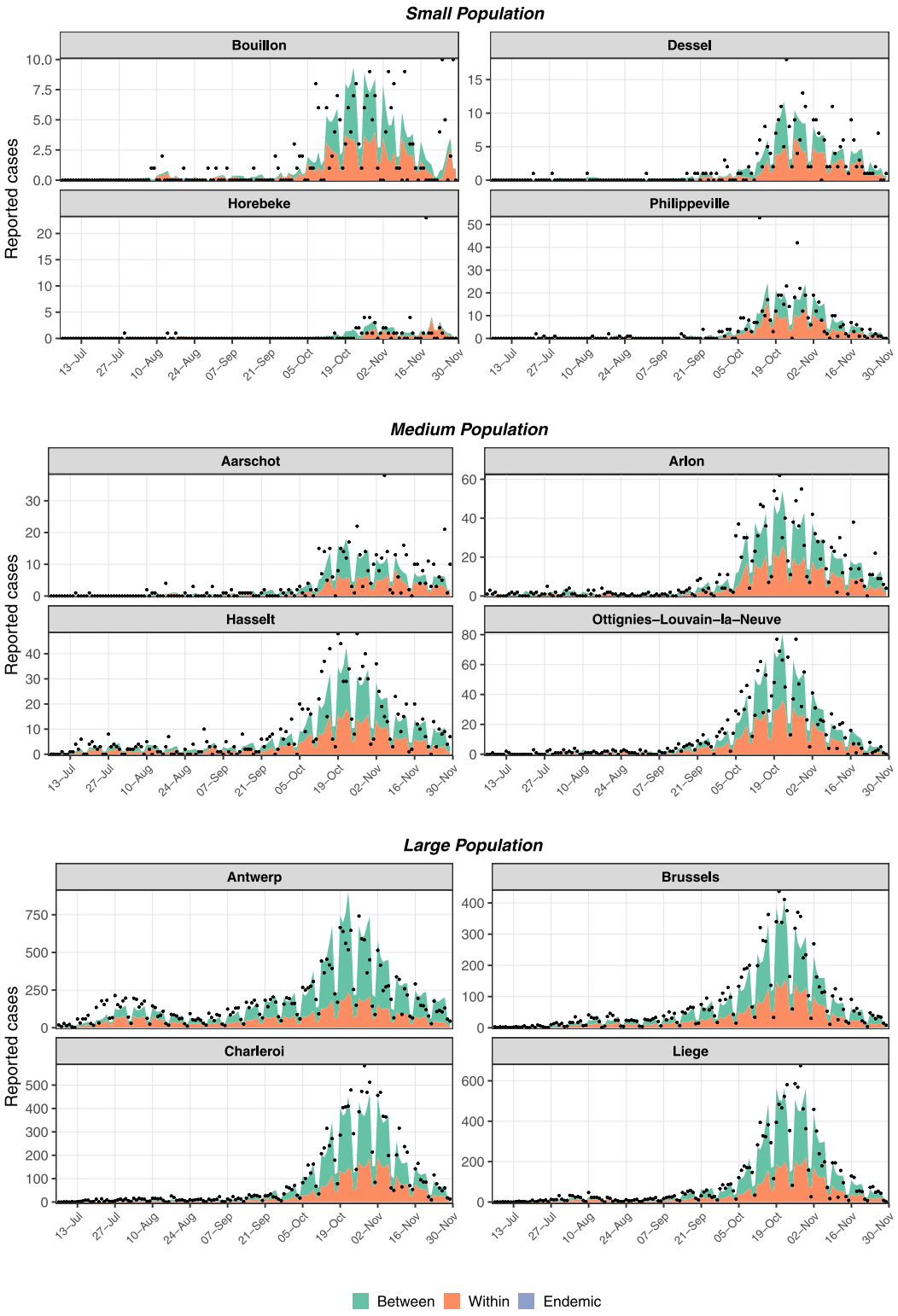

Fig. 6. Contribution of Endemic, Within- and Between-Municipality infection rates for randomly selected small (<10k), medium (>25k and <100k), and large (>100k) municipalities in terms of population size.

municipalities (e.g., cities), while the local component is more relevant in smaller (rural) municipalities.

The use of mobility data in spatial models to describe the connectivity amongst regions is gaining more and more attention in the literature. It should be noted that there are different connectivity matrices that can be defined based on mobile phone data, conditional on availability of the data. For example, Slater et al. (2022) define the spatial dependence through both physical proximity and mobility effect (Slater et al., 2022), while we define the connectivity based on the actual proportion of time spent in each municipality. A comparison of different definitions would be interesting for future research to give some guidance on best practices.

Incorporation of the mobility data in the spatio-temporal epidemic model indicated a fixed mobility weight to fit better than a time-varying

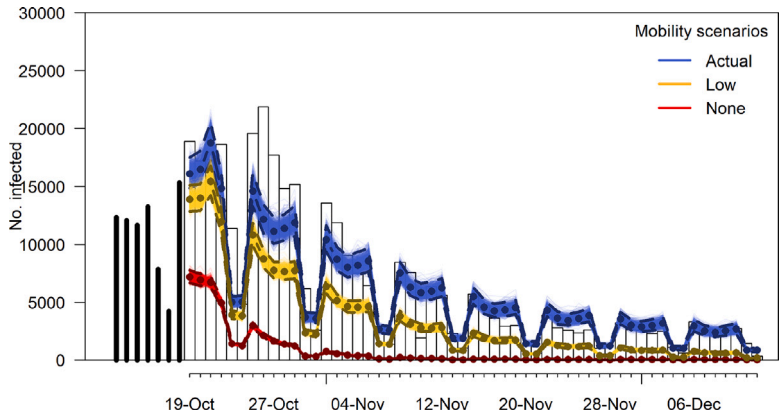

Fig. 7. Comparison of stochastic simulation predictions for the total number of infections using the actual observed mobility (Scenario 1), low mobility (Scenario 2), and assuming no mobility (Scenario 3).

weight. This points to the possibility that the reduction in mobility during the lockdown period was not significant enough to affect the transmission dynamics. Stochastic simulation however revealed that if the reduction of mobility during mid-October until December would have been similar to that during the lockdown of April/May, then a significant reduction in the number of new infections would have been observed.

This is our first attempt to encompass mobility data to construct spatial dependence in modeling epidemic spread. Our mobility data came from one telecom provider. Even though it holds the third largest market share in Belgium, its coverage is better in the Flemish Region while more variation is observed in the Walloon Region. In future projects, we will investigate whether additional data is available from multiple providers to assess the stability of mobility matrices.

We implemented the spatio-temporal epidemic model under the hhh4 framework supported in the package `surveillance`, where inference is made via maximum likelihood estimation. It is also straightforward to fit such model with Hierarchical Bayesian Modeling, as described in Wakefield et al. (2019). Based on the results from this study and available literature, we can set up informative priors and proceed in the Bayesian framework for future work.

The hhh4 model is also widely used for COVID-19 modeling. Examples can be found in Celani and Giudici (2022), Giuliani et al. (2020), Grimée et al. (2022) and Ssentongo et al. (2021). We illustrated our approach on the period from 29 June 2020 to 13 December 2020, which can easily be extended to longer periods and with the inclusion of other covariates, e.g. vaccine coverage. Testing capacity before this period was limited, and hence the observed epidemic curve did not reflect the real situation. Nevertheless, it is also difficult to completely rule out or precisely assess the impact of under-reporting within the considered time frame, and this is a limitation of our study. For future research, it would be interesting to study the impact of underreporting on the different components in the model, especially when the underreporting is time-varying (Bracher and Held, 2021).

The combination of mobility and social contact interventions implemented in Belgium clearly had an effect on the COVID-19 transmission dynamics. Further work is still required not only to completely disentangle the effect of different types of contacts in mobility and transmission pattern, but also to find the optimal balance between the negative effect of various interventions and the expected public health gain. Next to the impact of within-country mobility on the spread of COVID-19, investigation of the impact on incoming travel from other countries is still important.

Funding

NH and CF acknowledge support from the European Union's Horizon 2020 research and innovation programme - project EpiPose (Grant agreement number 101003688).

CRediT authorship contribution statement

Chellafe Ensoy-Musoro: Conceptualization, Methodology, Formal analysis, Writing – original draft. **Minh Hanh Nguyen:** Methodology, Formal analysis, Writing – original draft. **Niel Hens:** Conceptualization, Writing – review & editing. **Geert Molenberghs:** Writing – review & editing. **Christel Faes:** Conceptualization, Methodology, Formal analysis, Writing – original draft, Data collection.

Declaration of competing interest

The authors declare that they have no known competing financial interests or personal relationships that could have appeared to influence the work reported in this paper.

Data availability

The authors do not have permission to share data.

Acknowledgment

All authors have read and agreed to the published version of the manuscript

Appendix A. Supplementary data

Supplementary material related to this article can be found online at https://doi.org/10.1016/j.sste.2023.100568.

References

Anderson, R., Heesterbeek, H., Klinkenberg, D., Hollingsworth, T.D., 2020. How will country-based mitigation measures influence the course of the COVID-19 epidemic? Lancet Infect. Dis. 395 (10228), 931–934. http://dx.doi.org/10.1016/S0140-6736(20)30567-5.

Badr, H., Du, H., Marshall, M., Dong, E., Squire, M., Gardner, L., 2020. Association between mobility patterns and COVID-19 transmission in the USA: a mathematical modelling study. Lancet Infect. Dis. 20 (11), 1247–1254. http://dx.doi.org/10.1016/S1473-3099(20)30725-8.

Bajardi, P., Poletto, C., Ramasco, C.J., Tizzoni, M., Colizza, V., Vespignani, A., 2011. Human mobility networks, travel restrictions, and the global spread of 2009 H1N1 pandemic. PLoS One 6 (1), e16591. http://dx.doi.org/10.1371/journal.pone.0016591.

Bracher, J., Held, L., 2020. Endemic-epidemic models with discrete-time serial interval distributions for infectious disease prediction. Int. J. Forecast. http://dx.doi.org/10.1016/j.ijforecast.2020.07.002.

Bracher, J., Held, L., 2021. A marginal moment matching approach for fitting endemic-epidemic models to underreported disease surveillance counts. Biometrics 77 (4), 1202–1214. http://dx.doi.org/10.1111/biom.13371.

Celani, A., Giudici, P., 2022. Endemic–epidemic models to understand COVID-19 spatio-temporal evolution. Spat. Stat. 49, 100528. http://dx.doi.org/10.1016/j.spasta.2021.100528.

Coletti, P., Wambua, J., Gimma, A., Willem, L., Vercruysse, S., Vanhoutte, B., Jarvis, C.I., Van Zandvoort, K., Edmunds, J., Beutels, P., Hens, N., 2021. CoMix: comparing mixing patterns in the Belgian population during and after lockdown. Sci. Rep. 10, 21885, https://www.nature.com/articles/s41598-020-78540-7.pdf.

Cot, C., Cacciapaglia, G., Sannino, F., 2021. Mining Google and Apple mobility data: temporal anatomy for COVID-19 social distancing. Sci. Rep. 11, 4150. http://dx.doi.org/10.1038/s41598-021-83441-4.

Crisiscentrum, 2021. MB 23/03/2020–COVID-19. https://crisiscentrum.be/sites/default/files/content/mb_-_23-maart.pdf. (Accessed 11 May 2021).

Czado, C., Gneiting, T., Held, L., 2009. Predictive model assessment for count data. Biometrics 65 (4), 1254–1261. http://dx.doi.org/10.1111/j.1541-0420.2009.01191.x.

FOD Volksgezondheid, 2021. Coronavirus COVID-19. https://www.info-coronavirus.be/en/. (Accessed 11 May 2021).

Gatalo, O., Tseng, K., Hamilton, A., Lin, G., Klein, E., 2020. Associations between phone mobility data and COVID-19 cases. Lancet Infect. Dis. 21 (5), E111. http://dx.doi.org/10.1016/S1473-3099(20)30725-8.

Giuliani, D., Dickson, M.M., Espa, G., Santi, F., 2020. Modelling and predicting the spatio-temporal spread of COVID-19 in Italy. BMC Infect. Dis. 20 (1), 1–10. http://dx.doi.org/10.1186/s12879-020-05415-7.

Grimée, M., Dunbar, M.B.N., Hofmann, F., Held, L., 2022. Modelling the effect of a border closure between Switzerland and Italy on the spatiotemporal spread of COVID-19 in Switzerland. Spat. Stat. 49, 100552. http://dx.doi.org/10.1016/j.spasta.2021.100552.

Held, L., Höhle, M., Hofmann, M., 2005. A statistical framework for the analysis of multivariate infectious disease surveillance counts. Stat. Model. 5 (3), 187–199. http://dx.doi.org/10.1191/1471082X05st098oa.

Kraemer, M., Yang, C., Gutierrez, B., Wu, C., Klein, B., Pigott, D., Open Covid-19 Data Working Group, Du Plessis, L., Faria, N., Li, R., Hanage, W., Brownstein, J., Layan, M., Vespignani, A., Tian, H., Dye, C., Pybus, O., Scarpino, S., 2020. The effect of human mobility and control measures on the COVID-19 epidemic in China. Science 368 (6490), 493–497. http://dx.doi.org/10.1126/science.abb4218.

Liu, Y., Morgenstern, C., Kelly, J., Lowe, R., CMMID COVID-19 Working Group, Jit, M., 2021. The impact of non-pharmaceutical interventions on SARS-CoV-2 transmission across 130 countries and territories. BMC Med. 19, 40. http://dx.doi.org/10.1186/s12916-020-01872-8.

Meyer, S., Held, L., Höhle, M., 2017. Spatio-temporal analysis of epidemic phenomena using the R package surveillance. J. Stat. Softw. 77, 1–5. http://dx.doi.org/10.18637/jss.v077.i11.

Nouvellet, P., Bhatia, S., Cori, A., et al., 2021. Reduction in mobility and COVID-19 transmission. Nature Commun. 12, 1091. http://dx.doi.org/10.1038/s41467-021-21358-2.

Peak, C.M., Wesolowski, A., Zu Erbach-Schoenberg, E., Tatem, A.J., Wetter, E., Lu, X., Power, D., Weidman-Grunewald, E., Ramos, S., Moritz, S., Buckee, C.O., Bengtsson, L., 2018. Population mobility reductions associated with travel restrictions during the Ebola epidemic in Sierra Leone: use of mobile phone data. Int. J. Epidemiol. 47, 1562–1570. http://dx.doi.org/10.1093/ije/dyy095.

Pullano, G., Valdano, E., Scarpa, N., Rubrichi, S., Colizza, V., 2020. Evaluating the effect of demographic factors, socioeconomic factors, and risk aversion on mobility during the COVID-19 epidemic in France under lockdown: a population-based study. Lancet Digit. Health 2 (12), e638–e649. http://dx.doi.org/10.1016/S2589-7500(20)30243-0.

Sciensano, 2021. COVID-19 data. https://www.sciensano.be/en/covid-19-data. (Accessed 11 May 2021).

Slater, J.J., Brown, P.E., Rosenthal, J.S., Mateu, J., 2022. Capturing spatial dependence of COVID-19 case counts with cellphone mobility data. Spat. Stat. 49, 100540. http://dx.doi.org/10.1016/j.spasta.2021.100540.

Ssentongo, P., Fronterre, C., Geronimo, A., Greybush, S.J., Mbabazi, P.K., Muvawala, J., et al., 2021. Pan-African evolution of within-and between-country COVID-19 dynamics. Proc. Natl. Acad. Sci. 118 (28), e2026664118. http://dx.doi.org/10.1073/pnas.2026664118.

Turner, H., Firth, D., 2020. Generalized nonlinear models in R: An overview of the gnm package. R package version 1.1-1. https://cran.r-project.org/package=gnm.

Wakefield, J., Dong, T.Q., Minin, V.N., 2019. Spatio-temporal analysis of surveillance data. In: Handbook of Infectious Disease Data Analysis. Chapman and Hall/CRC, pp. 455–475.

World Health Organization, 2021. COVID-19 situation reports. https://www.who.int/emergencies/diseases/novel-coronavirus-2019/situation-reports. (Accessed 11 May 2021).

Zeng, C., Zhang, J., Li, Z., Sun, X., Olatosi, B., Weissman, S., Li, X., 2021. Spatial-temporal relationship between population mobility and COVID-19 outbreaks in South Carolina: Time series forecasting analysis. J. Med. Internet Res. 23 (4), e27045. http://dx.doi.org/10.2196/27045.

Zhang, J., Litvinova, M., Liang, Y., Wang, Y., Wang, W., Zhao, S., Wu, Q., Merler, S., Viboud, C., Vespignani, A., Ajelli, M., Yu, H., 2020. Changes in contact patterns shape the dynamics of the COVID-19 outbreak in China. Science 368 (6498), 1481–1486. http://dx.doi.org/10.1126/science.abb8001.